Journal of Infrastructure Intelligence and Resilience 4 (2025) 100170

Contents lists available at ScienceDirect

Journal of Infrastructure Intelligence and Resilience

journal homepage: www.journals.elsevier.com/journal-of-infrastructure-intelligence-and-resilience

Partial transfer matrix-based group sparse regularisation for impact force localization and reconstruction

Bing Zhang, Xinqun Zhu *, Zihao He, Jianchun Li

School of Civil and Environmental Engineering, University of Technology Sydney, Ultimo, NSW, 2007, Australia

ARTICLE INFO

Handling Editor: Ms. Yanwei Li

Keywords:
Impact force identification
Partial transfer matrix
Group sparse regularisation
One single sensor

ABSTRACT

Existing methods for impact force identification are based on full transfer matrix. Constructing and using transfer matrices can be computationally intensive, especially for large-scale complex structures in practice. Partial transfer matrix refers to a subset of the full transfer matrix, potentially reducing computational cost and complexity. In this paper, a partial transfer matrix-based group sparse regularisation method is proposed for the impact force localization and reconstruction. Its robustness and adaptivity with respect to different subsets of full transfer matrix, noise level and number of impact forces are numerically studied using impact forces on a simply supported beam. The number of sensors for impact force identification can be significantly reduced by the proposed method and its localization and time history reconstruction can be determined even with one single sensor configuration. A 10 m long steel-concrete composite bridge model is built in the laboratory. The effectiveness of the proposed method for impact force identification is validated and compared with L_1-norm and L_2-norm regularisation methods numerically and experimentally. Results show that the proposed partial transfer matrix-based group sparse regularisation method has good robustness and identification accuracy and has better performance on the impact force localization and time history reconstruction comparing with L_1-norm and L_2-norm regularisation methods.

1. Introduction

Impact force identification regarding to force localization and reconstruction is an essential task in civil engineering for assessing structural loading condition, structural health monitoring, and reliability design (LeClerc et al., 2007; Park et al., 2009; Jia et al., 2015a; Khanam et al., 2015). In practice, it is often difficult, even impossible to measure all forces on the entire structure directly using force transducers. Force identification as an indirect measurement has been studied over last few decades, in which the easily measurable structural vibration responses are used to identify impact forces (Liu et al., 2021; Sanchez and Benaroya, 2014; Inoue et al., 2001). It is an inverse problem to estimate the force locations and amplitudes from structural dynamic responses, e.g. displacement, velocity, acceleration and strain responses, etc. The ill-posedness of impact force identification problems makes it exceedingly challenging to provide a unique and stable solution and often results in large estimation errors. Unknown excitation locations further exacerbate the difficulty of force identification.

Regularisation techniques, such as Tikhonov regularisation (also known as the L_2-norm regularisation method) and the sparse regularisation techniques, are widely used to solve the ill-posedness in inverse problems. Zhu and Law (2002) used Tikhonov regularisation to identify moving loads on a continuous beam from measured structural responses. Jacquelin et al. (2003) compared the performance of Tikhonov regularisation and truncated singular value decomposition for reconstructing the time history of impact force acting on an aluminium plate in time domain. Jia et al. (2015b) proposed a weighted Tikhonov regularisation method for identifying random dynamic force in the frequency domain, where the weighting matrix depends on the frequency response function. Sparse regularisation has received considerable interest on the field of signal recovery. The L_1-norm regularisation as the standard sparse regularisation is widely used for dynamic force identification. Qiao et al. (2019a) proposed an enhanced sparse regularisation method for impact force identification based on weighted L_1-norm minimization. To consider the intrinsic structure of the impact force that nonzero elements occur in groups, sparse group regularisation method based on minimizing the mixed $L_{2,1}$-norm norm is proposed for impact force identification (Qiao et al., 2019b). These above studies are based on the

This article is part of a special issue entitled: ANSHM published in Journal of Infrastructure Intelligence and Resilience.

* Corresponding author.
E-mail address: xinqun.zhu@uts.edu.au (X. Zhu).

https://doi.org/10.1016/j.iintel.2025.100170
Received 25 June 2025; Received in revised form 12 August 2025; Accepted 17 August 2025
Available online 20 August 2025

assumption that the locations of impact forces are exactly known.

In practice, the locations of impact forces are often unknown, that makes the force identification process even more challenging. A variety of approaches have been proposed to tackle the force localization and reconstruction problem. Wang and Chiu (2003) identified the location and amplitude of an unknown impact force acting on a simply supported beam in time and frequency domain. Kalhori et al. (2018) applied the Tikhonov regularisation method for reconstructing the time history and localization of impact force acting on a composite panel. Goutaudier et al. (2020) proposed a single sensor technique for localizing and reconstructing impact events on structures. Qiu et al. (2019) combined pattern recognition with the similarity metric to localize impacts in time domain. After the localization, the impact time history was reconstructed with Tikhonov regularisation. Li and Lu (2016) proposed a method for localization and identification of impact. The location of impact was first determined with an error functional indicator using the complex method. The identification of impact time history was then considered as a constrained optimization problem. Wambacq et al. (2019) presented an algorithm to localize and identify forces in the frequency domain. Recently group sparsity has been exploited as an alternative sparse regularisation technique for solving impact force identification problems. Feng et al. (2021) utilized the external force group sparse feature and developed a group relevance vector machine group sparsity regularisation method to localize and reconstruct external forces on structures using structure responses in time domain. Liu et al. (2022) also used the force vector group sparse feature and proposed a novel impact force identification method based on the nonconvex overlapping group sparsity (NOGS), allowing to localize the impact force and recover its time history simultaneously from a limited number of measurements. In all above studies, the general full transfer matrix was used, and it required the force information of the whole time period including both loading and unloading periods. In practice, the number of sensors may be limited, and the situation where the number of sensors is less than the number of excitations faces the underdetermined issue. For full-scale structures, the transfer matrix for the whole time period is a high-dimensional matrix. The corresponding computational cost for the force identification is high, especially dealing with the data storage and inverse calculation. For the force identification, the information before and after the impact force in the full transfer matrix was redundant. This redundancy induces the ill-posedness of the inverse problem for the force identification, and it significantly affects accuracy of the force identification.

To address the above limitations, the partial transfer matrix is proposed for impact force identification in this study. By using the prior information of impact force, the information including a short time period and excitation time can be obtained from measured responses. Then a partial transfer matrix associated with the time period can be constructed. This approach offers two advantages. First, it significantly reduces the dimensionality of the problem, improving computational efficiency. Second, it reduces the unnecessary data, enhancing the accuracy of the solution.

In this paper, a partial transfer matrix-based group sparse regularisation method for impact force localization and reconstruction is proposed. It is organized as follows: Section 2 presents the preliminary theories for impact force identification. In Section 3, the proposed impact force identification method based on partial transfer matrix and group sparse regularisation are depicted. Numerical and experimental validation are studied in Sections 4 and 5, respectively. Finally, some conclusions are drawn in Section 6.

2. Preliminary theories for impact force identification

2.1. Dynamics of a simply supported beam under external forces

For a simply supported uniform Euler-Bernoulli beam under external forces, its dynamic governing equation can be given as:

$$\boldsymbol{M}\ddot{\boldsymbol{u}}(t)+\boldsymbol{C}\dot{\boldsymbol{u}}(t)+\boldsymbol{K}\boldsymbol{u}(t)=\boldsymbol{L}\boldsymbol{F}(t) \tag{1}$$

where $\boldsymbol{M}$, $\boldsymbol{C}$ and $\boldsymbol{K}$ are the mass, damping, and stiffness matrices of the beam respectively; $\ddot{\boldsymbol{u}}(t)$, $\dot{\boldsymbol{u}}(t)$ and $\boldsymbol{u}(t)$ are acceleration, velocity and displacement responses of the beam at time t, respectively; $\boldsymbol{F}(t)$ is the input force vector and $\boldsymbol{L}$ is the mapping matrix.

Eq. (1) can be expressed in the state space form as,

$$\dot{\boldsymbol{z}}(t)=\boldsymbol{A}\boldsymbol{z}(t)+\boldsymbol{B}\boldsymbol{F}(t) \tag{2}$$

where $\boldsymbol{z}(t)=\begin{Bmatrix}\boldsymbol{u}(t)\\ \dot{\boldsymbol{u}}(t)\end{Bmatrix}$, $\boldsymbol{A}=\begin{bmatrix}\boldsymbol{0} & \boldsymbol{I}\\ -\boldsymbol{M}^{-1}\boldsymbol{K} & -\boldsymbol{M}^{-1}\boldsymbol{C}\end{bmatrix}$, and $\boldsymbol{B}=\begin{bmatrix}\boldsymbol{0}\\ \boldsymbol{M}^{-1}\boldsymbol{L}\end{bmatrix}$. $\boldsymbol{A}$ is the continuous system matrix; $\boldsymbol{B}$ is the input matrix and $\boldsymbol{I}$ is an identity matrix. When acceleration response measurements are available at certain locations of the structure, the output vector can be formulated as $\boldsymbol{y}(t)=\mathbf{R}\ddot{\boldsymbol{u}}(t)$ with $\mathbf{R}$ being the output influence matrix and depending on the sensor locations. Consequently, the measurement can be expressed as

$$\boldsymbol{y}(t)=\boldsymbol{C}\boldsymbol{z}(t)+\boldsymbol{D}\boldsymbol{F}(t) \tag{3}$$

where $\boldsymbol{C}=\left[-\boldsymbol{R}\boldsymbol{M}^{-1}\boldsymbol{K},-\boldsymbol{R}\boldsymbol{M}^{-1}\boldsymbol{C}\right]$ and $\boldsymbol{D}(t)=\boldsymbol{R}\boldsymbol{M}^{-1}\boldsymbol{L}$ are respectively the continuous output matrix and feedthrough matrix.

Combining Eqs. (2) and (3), we can obtain the continuous analytical solution as,

$$\boldsymbol{y}(t)=\boldsymbol{C}\boldsymbol{\Phi}(t)\boldsymbol{z}(0)+\boldsymbol{C}\int_0^t\boldsymbol{\Phi}(t,\tau)\boldsymbol{B}\boldsymbol{F}(\tau)d\tau+\boldsymbol{D}\boldsymbol{F}(t) \tag{4}$$

where $\boldsymbol{\Phi}(t)=\exp(\boldsymbol{A}t)$; $\boldsymbol{z}(0)$ is the initial dynamic condition of the beam.

An impact dynamic force $\boldsymbol{F}_i(t)$ is represented as,

$$\boldsymbol{F}_i(t)=\boldsymbol{e}_i\delta(t-\tau),\text{ with }\boldsymbol{e}_i=[0,\cdots,0,1,0,\cdots,0]^T \tag{5}$$

Considering the zero initial conditions, the measured dynamic response at the jth location of the beam is

$$h_{ji}(t,\tau)=y_j(t)=\boldsymbol{C}_j\int_0^t\boldsymbol{\Phi}(t,\tau)\boldsymbol{B}\boldsymbol{e}_i\delta(\tau-\tau_1)d\tau+\boldsymbol{D}\boldsymbol{e}_i\delta(t-\tau_1) \tag{6}$$

For multiple impact forces and measured responses, Eq. (6) can be rewritten as,

$$\boldsymbol{y}(t)=\int_0^t\boldsymbol{h}(t,\tau)\boldsymbol{F}(\tau)d\tau \tag{7}$$

where $\boldsymbol{h}(t,\ \tau)=\begin{bmatrix}h_{11}(t,\tau) & h_{12}(t,\tau) & \ldots & h_{1,nr}(t,\tau)\\ h_{21}(t,\tau) & h_{22}(t,\tau) & \cdots & h_{2,nr}(t,\tau)\\ \ldots & \ldots & \cdots & \ldots\\ h_{ns,1}(t,\tau) & h_{ns,2}(t,\tau) & \cdots & h_{ns,nr}(t,\tau)\end{bmatrix}$; $\mathbf{F}(t)=[F_1(t),F_2(t),\cdots,F_{nr}(t)]^T$; ns is the number of sensors; nr is the number of impact forces applied asynchronously at different locations.

The convolution problem of Eq. (7) can be converted into the discretised form as,

$$\mathbf{Y}=\mathbf{H}\mathbf{F} \tag{8}$$

where $=\begin{Bmatrix}\mathbf{Y}_1\\ \mathbf{Y}_2\\ \vdots\\ \mathbf{Y}_{ns}\end{Bmatrix}$, $\mathbf{H}=\begin{bmatrix}\mathbf{H}_{11} & \mathbf{H}_{12} & \cdots & \mathbf{H}_{1,nr}\\ \mathbf{H}_{21} & \mathbf{H}_{22} & \cdots & \mathbf{H}_{2,nr}\\ \vdots & \vdots & \ddots & \vdots\\ \mathbf{H}_{ns,1} & \mathbf{H}_{ns,2} & \cdots & \mathbf{H}_{ns,nr}\end{bmatrix}$ and $\mathbf{F}=\begin{Bmatrix}\mathbf{F}_1\\ \mathbf{F}_2\\ \vdots\\ \mathbf{F}_{nr}\end{Bmatrix}$

$$\mathbf{H}_{11} = \begin{bmatrix} h_{11}(t_1) & 0 & \cdots & 0 & 0 \\ h_{11}(t_2) & h_{11}(t_1) & \cdots & 0 & 0 \\ \vdots & \vdots & \cdots & \vdots & \vdots \\ h_{11}(t_{n-1}) & h_{11}(t_{n-2}) & \cdots & h_{11}(t_1) & 0 \\ h_{11}(t_n) & h_{11}(t_{n-1}) & \cdots & h_{11}(t_2) & h_{11}(t_1) \end{bmatrix} \Delta t \tag{9}$$

Considering a single impact force that may applied at one of the *nr* potential pre-defined locations, the assembled force $\boldsymbol{F}$ can be formed into *nr* subgroups, corresponding to each of the force locations. For *ns* measurements, an illustration for impact force identification in the matrix form of Eq. (8) is shown in Fig. 1 when the non-zero impact force vector $\boldsymbol{F}_1$ is applied. From the figure, only a fraction of elements in $\boldsymbol{F}$ is exerted by non-zero values, which is referred as the true force location. The rest of them are referred as non-force locations. For traditional force identification methods, the general whole transfer matrix is used for force identification by solving the inverse problem, and the number of sensors should be more than the number of forces to avoid the under-determined situation.

2.2. Impact force identification based on traditional L_2-norm and L_1-norm regularisation techniques

The impact response matrix as shown in Fig. 1 is ill-posed that means that the measurement noise would be amplified significantly by the least squares estimate using Eq. (8). Therefore, regularisation techniques have been used to stabilise the solution for impact force identification. The Tikhonov regularisation based on minimizing L_2-norm and sparse regularisation based on minimizing L_1-norm are two popular regularisation techniques for solving the inverse problem of ill-posed and large-scale matrices. For Tikhonov L_2-norm regularisation, it seeks for a stable solution by introducing an L_2-norm penalty with controlling highly oscillating components. Hence, the impact force identification problem defining as a trade-off between the residual and regularized norms,

$$\underset{\boldsymbol{F}}{\text{minimize}} \; \|\mathbf{HF} - \mathbf{y}\|_2^2 + \lambda \|\boldsymbol{F}\|_2^2 \tag{10}$$

where $\lambda > 0$ is the regularisation parameter. The L_2-norm of the impact force $\|\boldsymbol{F}\|_2^2$ is called the regularisation term or the penalty term. Here, the ill-posed model in Eq. (8) is improved by introducing an additional term in Eq. (10), that renders the problem less sensitive to perturbations. Due to the convexity of Eq. (10), Tikhonov regularisation has an analytic solution with any fixed λ

$$\mathbf{F} = \left(\mathbf{H}^{\mathrm{T}}\mathbf{H} + \lambda \mathbf{I}\right)^{-1}\mathbf{H}^{\mathrm{T}}\mathbf{y} \tag{11}$$

From Eq. (11), the Tikhonov solution is a smooth function of λ as it varies over the interval $(0, \infty)$.

On the other hand, the Lasso regression based on L_1-norm are widely used in domains with massive datasets, such as genomics, where efficient and fast algorithms are essential. The Lasso is, however, not robust to high correlations among predictors and will arbitrarily choose one and ignore the others and break down when all predictors are identical. The Lasso penalty expects many coefficients to be close to zero, and only a small subset to be larger (and nonzero). The Lasso estimator uses the L_1 penalized least squares criterion to obtain a sparse solution to the following optimization problem.

$$\underset{\boldsymbol{F}}{\text{minimize}} \; \|\mathbf{HF} - \mathbf{y}\|_2^2 + \lambda \|\mathbf{F}\|_1 \tag{12}$$

For the impact force identification, the pulse interval can be regarded as a group and the sparse elements of unknown impact forces exhibit intrinsic structure in form of groups as shown in Fig. 1. The above standard sparse regularisation techniques have not considered the group structure of impact forces.

3. Impact force identification using group sparse regularisation

In this section, an impact force identification method based on group sparse regularisation is proposed using one sensor to identify the locations and amplitudes of the forces. The method is based on the partial transfer matrix and group sparse regularisation from the acceleration response of a single sensor.

3.1. Impact force identification using one single sensor

Fig. 2 shows a simple supported Euler-Bernoulli beam subjected to impact forces. The locations of impact forces are unknown and *nr* potential force locations are pre-defined.

When the response measured from one sensor is used for the impact force identification, the discrete form of Eq. (8) can be illustrated in

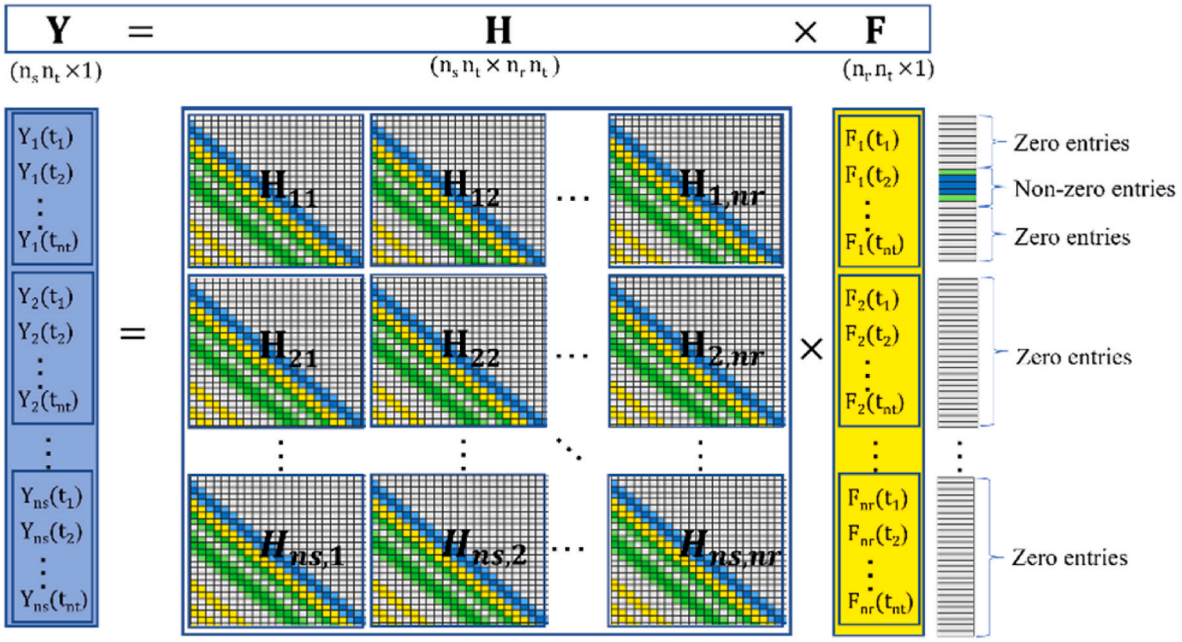

Fig. 1. The illustration of force identification problem in matrix form.

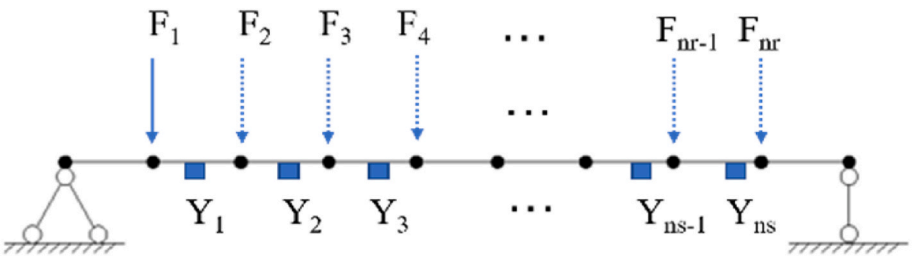

Fig. 2. Simply supported beam subjected to impact forces.

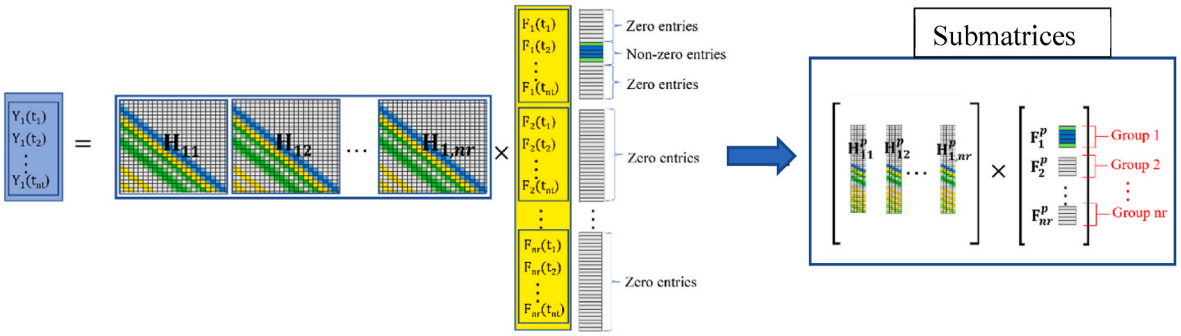

Fig. 3. The discrete form using the submatrix with one single sensor.

Fig. 3. The M, C, K matrices are pre-known, which are used to construct the full transfer matrix. Based on the intrinsic feature of the impact force as shown in Fig. 3, only a submatrix of the general full transfer matrix is associated with the impact force time interval and this submatrix could be selected for the force identification. The dimension of the submatrix is much smaller than that of the general transfer matrix and the computational efficiency could be increased significantly.

For the case with one single sensor, the inverse problem of impact force identification can be expressed as

$$\mathbf{Y_1} = \mathbf{HP} \tag{13}$$

Assuming there is non-zero value in some specific time points of the impact force history. The matrix $\mathbf{H}$ and $\mathbf{F}$ can be divided into submatrix according to whether the force value equals to 0.

$$\mathbf{H} = \begin{bmatrix} \mathbf{H}^o_{11} & \mathbf{H}^p_{11} & \mathbf{H}^q_{11} & \mathbf{H}^o_{12} & \mathbf{H}^p_{12} & \mathbf{H}^q_{12} & \cdots & \mathbf{H}^q_{1,nr} \\ \mathbf{H}^o_{21} & \mathbf{H}^p_{21} & \mathbf{H}^q_{21} & \mathbf{H}^o_{22} & \mathbf{H}^p_{22} & \mathbf{H}^q_{22} & \cdots & \mathbf{H}^q_{2,nr} \\ \vdots & \vdots & \vdots & \vdots & \vdots & \vdots & \ddots & \vdots \\ \mathbf{H}^o_{ns,1} & \mathbf{H}^p_{ns,1} & \mathbf{H}^q_{ns,1} & \mathbf{H}^o_{ns,2} & \mathbf{H}^p_{ns,2} & \mathbf{H}^q_{ns,2} & \cdots & \mathbf{H}^q_{ns,nr} \end{bmatrix} \tag{14}$$

$$\mathbf{F} = \left\{ \mathbf{F}_1^{o\mathrm{T}} \quad \mathbf{F}_1^{p\mathrm{T}} \quad \mathbf{F}_1^{q\mathrm{T}} \quad \mathbf{F}_2^{o\mathrm{T}} \quad \mathbf{F}_2^{p\mathrm{T}} \quad \mathbf{F}_2^{q\mathrm{T}} \quad \cdots \quad \mathbf{F}_{\boldsymbol{nr}}^{q\ \mathrm{T}} \right\}^{\mathrm{T}} \tag{15}$$

where $\mathbf{F}_i^p$ denotes the force history vector with non-zero value at the location i, $\mathbf{F}_i^o$ and $\mathbf{F}_i^q$ denote the zero values vector. Hence,

$$\begin{aligned} \mathbf{Y}_j &= \mathbf{H}^o_{j1}\mathbf{F}^o_1 + \mathbf{H}^p_{j1}\mathbf{F}^p_1 + \mathbf{H}^q_{j1}\mathbf{F}^q_1 + \mathbf{H}^o_{j2}\mathbf{F}^o_2 + \mathbf{H}^p_{j2}\mathbf{F}^p_2 + \mathbf{H}^q_{j2}\mathbf{F}^q_2 + \cdots + \mathbf{H}^q_{j,nr}\mathbf{F}^q_{\boldsymbol{nr}} \\ &= \mathbf{H}^p_{j1}\mathbf{F}^p_1 + \mathbf{H}^p_{j2}\mathbf{F}^p_2 + \cdots + \mathbf{H}^p_{j,nr}\mathbf{F}^p_{\boldsymbol{nr}} \end{aligned} \tag{16}$$

Eq. (14) can be written as a matrix style:

$$\mathbf{Y}_1 = \mathbf{H}^p\mathbf{F}^p \tag{17}$$

where $\mathbf{H}^p = \begin{bmatrix} \mathbf{H}^p_{11} & \mathbf{H}^p_{12} & \cdots & \mathbf{H}^p_{1,nr} \end{bmatrix}$ is the partial transfer matrix, and the force vector is grouped as $\mathbf{F}^p = \begin{bmatrix} \mathbf{F}_1^{p\mathrm{T}} & \mathbf{F}_2^{p\mathrm{T}} & \cdots & \mathbf{F}_{nr}^{p\ \mathrm{T}} \end{bmatrix}^{\boldsymbol{T}}$.

Since an impact force often causes a large amplitude of the beam responses, the time interval and duration of the impact force can be estimated from responses to determine the partial transfer matrix. A threshold of the response value could be used to estimate the start time of the impact force. In practice, response measurements are inevitably contaminated by noise. Eq. (13) becomes,

$$\mathbf{Y}_1 = \mathbf{H}^p\mathbf{F}^p + \mathbf{w} \tag{18}$$

where the vector $\mathbf{w}$ represents the measurement noise.

3.2. *Partial transfer matrix based group sparse regularisation for impact force identification*

In this section, the incorporation of partial transfer matrix and group sparse regularisation technique for impact force identification is introduced. For impact force identification, the pulse interval can be regarded as a group and the sparse elements of unknown impact forces exhibit intrinsic structure in form of groups as shown in Fig. 3. To utilise the group structure, the group sparse regularisation technique for impact force identification is proposed and the $L_{2,1}$-norm penalty is used to replace the pure L_2-norm term in Eq. (10) or the L_1-norm penalty in Eq. (12). In the impact force identification from the response of one single sensor with an assumption of nr potential force locations, we have the response $\mathbf{Y_1} \in \mathbb{R}^{nt}$, a $nt \times (nr \cdot nt')$ matrix $\mathbf{H}^p$ and a vector $\mathbf{F}^p \in \mathbb{R}^{nr \cdot nt'}$. $nt' = 2m + n$, n denotes the nonzero values and m means the length before or after the force. Therefore, the problem can be generalised as an unconstrained optimization form,

$$\underset{\boldsymbol{F}}{\text{Minimize}} \ \|\mathbf{H}^p\mathbf{F}^p - \mathbf{Y}_1\|_2^2 + \lambda \sum_{i=1}^{nr} \left\|\mathbf{F}_i^p\right\|_2 \tag{19}$$

For solving this constrained optimization problem given in Eq. (19) falls in the class of gradient-projection methods, a common variant of gradient-projection methods computes a direction of descent at iterate k by finding the Euclidean-norm projection of a scaled steepest descent direction onto the feasible set. A spectral projected gradient algorithm (SPG) is adopted here (Meier et al., 2008). To describe the optimization procedure using the algorithm, the objective function $\|\mathbf{H}^p\mathbf{F}^p - \mathbf{Y}_1\|_2^2 + \lambda \sum_{i=1}^{nr} \left\|\mathbf{F}_i^p\right\|_2$ is denoted as $f(\boldsymbol{x})$ and $\boldsymbol{x}$ denotes the variable corresponding

to the force vector. Therefore, the values of the objective function and its gradient at iterate k can be represented as $f(\boldsymbol{x}_k)$ and $\nabla f(\boldsymbol{x}_k)$, respectively. Using Π to denote this projection, β as the scale factor for the steepest descent direction $\mathbf{d}$, and t as a step length, the iterates can be written as: $\boldsymbol{x}_{k+1} = \boldsymbol{x}_k + t(\prod(\boldsymbol{x}_k - \beta\nabla f(\boldsymbol{x}_k)) - \boldsymbol{x}_k)$. The descent direction is $\mathbf{d} \triangleq \prod(\boldsymbol{x}_k - \beta\nabla f(\boldsymbol{x}_k)) - \boldsymbol{x}_k$. The step length β determined using 'Barzilai and Borwein' (BB) algorithm is chosen as in the inverse Raliegh quotient $\beta = \frac{\boldsymbol{s}^T\boldsymbol{s}}{\boldsymbol{s}^T\boldsymbol{y}}$ (where $\boldsymbol{S} = \boldsymbol{x}_k - \boldsymbol{x}_{k-1}$; $\boldsymbol{y} = \nabla f(\boldsymbol{x}_k) - \nabla f(\boldsymbol{x}_{k-1})$) (Barzilai and Borwein, 1988). The step length t can be determined with a non-monotone Armijo line search (Armijo, 1966). In general, using the SPG strategy yields an algorithm that can efficiently compute the optimal projection by solving a small linearly constrained problem for each group. The detail procedure regarding to the algorithm can be found in the reference (Meier et al., 2008).

3.3. Determine the location of the impact force

When the forces for each group are identified, they can be used to identify the true force locations from all the potential locations. A location index can be calculated by the ratio between the norm of the estimated ith group force vector and that of the entire force vector in percentage defined as,

$$LOC_i = \frac{\|\tilde{\mathbf{F}}_i^p\|_2}{\|\tilde{\mathbf{F}}^p\|_2} \times 100\% \tag{20}$$

where $\tilde{\mathbf{F}}_i^p$ is the ith group of the estimated force vector, $\tilde{\mathbf{F}}^p$ is the entire estimated force vector. From Eq. (20), the location index for a certain force group with a largest value indicates the most possible true location of the impact force. Fig. 4 shows the flowchart of the proposed method.

4. Numerical study

4.1. Model description

To verify the effectiveness and performance of the proposed method for impact force identification, numerical simulations are carried out on a simply supported beam model. The beam model is 6 m long with the cross section of 0.1m × 0.03m and the mass density of 7850 kg/m^3. The Young's modulus E of the beam material is 2.05 × 10^{11}N/m^2. The Rayleigh damping is considered with two coefficients α = 0.5, β = 1 in this section. In practice, these two coefficients could be estimated using the damping ratios and natural frequencies of two vibration modes. The beam model is divided into 300 equal Euler-Bernoulli finite elements. The dynamic response of the beam under the impact force is calculated with a time interval of 0.001s and the time record duration of 4 s. The impact force is simulated as a triangular pulse with 5 nonzero values. The range of the impact force with nonzero values is identified. Nine possible force locations evenly distributed along the beam with the interval of 0.6 m are considered in the force localization, noted as P1∼P9. These locations are uniformly distributed along the beam as shown in Fig. 2. The distance between two adjacent locations is 0.6 m. The sensor

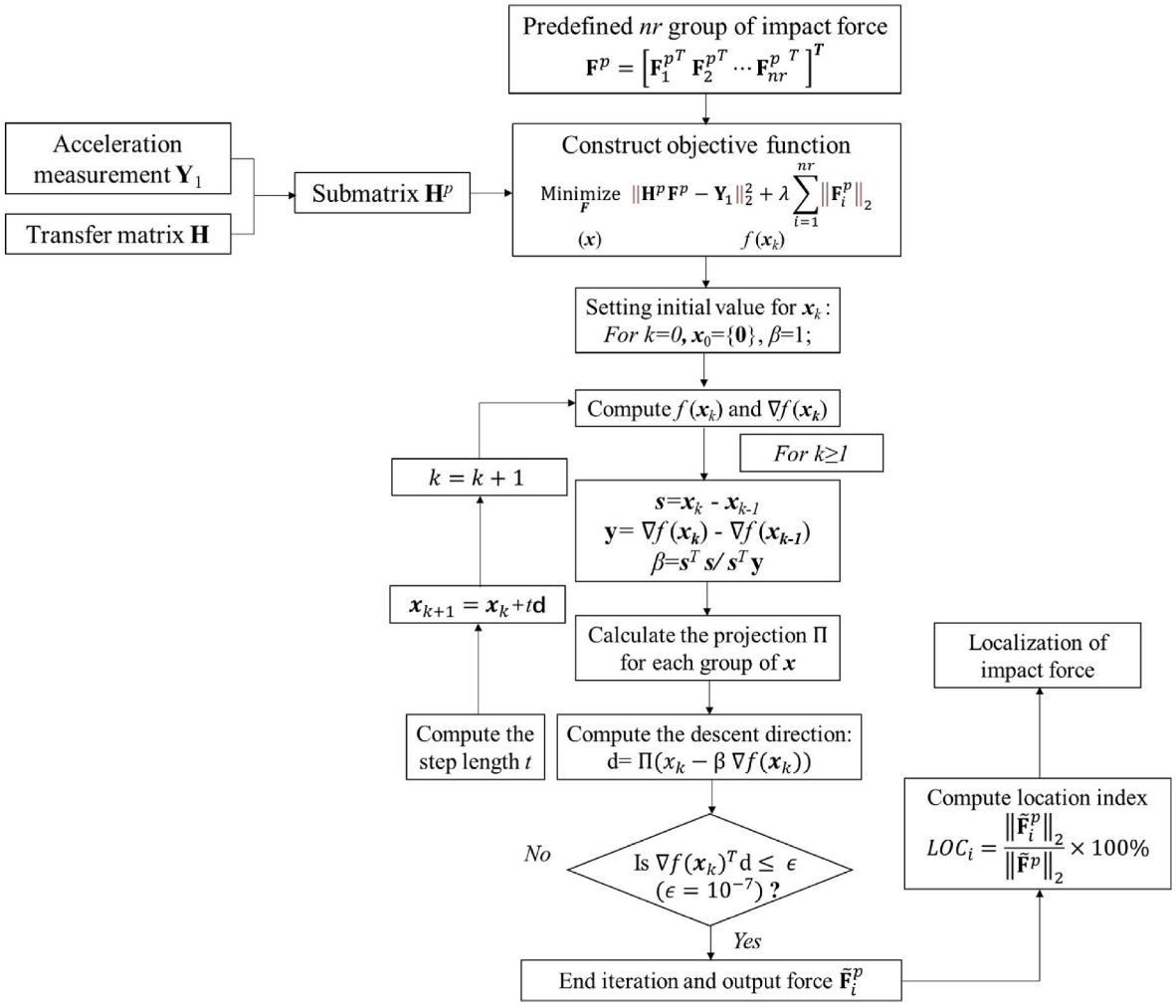

Fig. 4. Flowchart of the proposed method for force identification.

location does not have much effect on the identification result and the response Y_1 is used as arbitrary in this study.

To evaluate the accuracy of the impact force identification using the proposed method, the relative error (RE) for the ith force identification is defined as the difference between the actual force vector $\mathbf{F}_i^p$ and the estimated one $\widetilde{\mathbf{F}}_i^p$,

$$RE_i = \frac{\left\|\mathbf{F}_i^p - \widetilde{\mathbf{F}}_i^p\right\|_1}{\left\|\mathbf{F}_i^p\right\|_1} \times 100\% \tag{18}$$

To evaluate the accuracy of the peak value of the identified impact forces, the relative percentage error of the peak value (PRE) for the ith force identification is defined as

$$PRE_i = \frac{\left\|\mathbf{F}_{pi}^p - \widetilde{\mathbf{F}}_{pi}^p\right\|_1}{\left\|\mathbf{F}_{pi}^p\right\|_1} \times 100\% \tag{19}$$

where $\widetilde{\mathbf{F}}_{pi}^p$ and $\mathbf{F}_{pi}^p$ are the peak values of ith identified and true impact forces respectively.

In the simulations, the impact force is applied at location P2. The response of one single sensor (Y_1) is used. To study the effect of measurement noise, the white noise is added to simulate the measurement as,

$$\mathbf{Y}_n = \mathbf{Y}_1 + lev \times \frac{1}{n}\sum_{i=1}^{n} |\mathbf{Y}_1| \times \boldsymbol{rand} \tag{20}$$

where $\mathbf{Y}_n$ and $\mathbf{Y}_1$ are the structural responses corresponding to noise and noiseless, respectively. n is the total number of elements in the vector $\mathbf{Y}_1$. lev is the noise level. $\boldsymbol{rand}$ is a standard normal distribution vector. 5 % noise is added to the response to simulate the polluted measurement, unless otherwise specified.

4.2. Impact force identification

Based on the specific feature of the impact force and its relevant dynamic response, the duration of the impact force can be estimated as shown in Fig. 5. From the acceleration response, the force duration is around the beginning of the response marked as two red dotted lines in the figure. Based on this prior information, a suitable submatrix from the transfer matrix could be selected to identify the predefined locations force in this study. The data length of the submatrix depends on the time interval of the impact force and the sampling frequency. Assuming that the impact force is a triangular pulse with a short time interval of 0.006 s and there are 5 nonzero values, the 2 m +5 values around the beginning of the response are chosen to cover the excitation time interval of impact force, as shown in Fig. 5. The effects of the m value will be discussed in the later subsection.

Fig. 6 shows the identified results using the submatrix with $m = 5$ by the L_1-norm, L_2-norm regularisation methods and the proposed method, respectively. The identified impact force locations by these three methods are shown in Fig. 7(a)–(c), respectively and the reconstructed time histories of the impact force are shown in Fig. 7(d)-7(f), respectively. The force vector is separated into 9 groups, each associated with one potential force location. Among the potential locations, only nonzero forces occur at the true force location. From Fig. 6, the identified result by the proposed method is agree well with the true value, and that by the L_1-norm regularisation method is close to the true value with some small oscillations. There are large oscillations in the result by the L_2-norm regularisation method and it fails to reconstruct the impact force. In Fig. 7, all three methods could indicate the location of the impact force, but the result by the L_2-norm regularisation has some large LOC values at false force locations. The LOC values by the L_1-norm and $L_{2,1}$-norm regularisation methods are approximate 100 % at the force location and the values at other locations are close to zero and the results show that the impact force location could be identified accurately using these two methods. Fig. 7(d) shows that the reconstructed impact force by the L_2-norm regularisation method has large errors compared to the true value, and the RE and PRE values are 80.51 % and 57.82 % respectively. In Fig. 7(e), the identified result by the L_1-norm regularisation method has some oscillations around the force peak, and the RE and PRE values are 20.91 % and 4.90 % respectively. From Fig. 7(f), the result by the proposed $L_{2,1}$-norm regularisation method fits well with the true force, and the RE and PRE values are 1.06 % and 0.15 % respectively. From the above, the impact force location and values could be accurately identified simultaneously with one single sensor by the proposed partial transfer matrix-based group sparse regularisation method.

4.3. Effects of the m value

The selection of m value is to ensure that the required time steps of the impact excitation are included and it determines the size of the partial transfer matrix. In this study, the m value is selected from 0 to 30. Different partial transfer matrices based on the m value are constructed for impact force identification using the proposed method. The

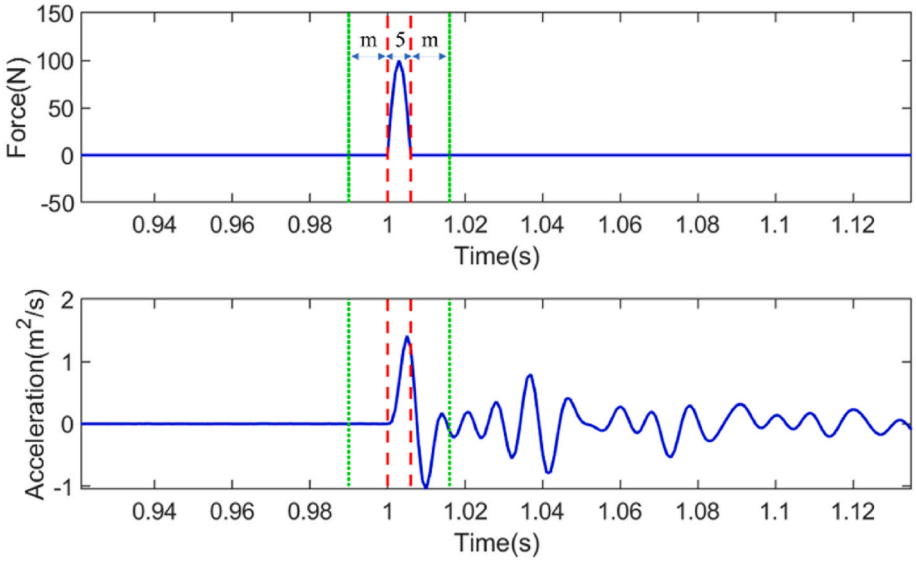

Fig. 5. Impact excitation interval determination from acceleration responses.

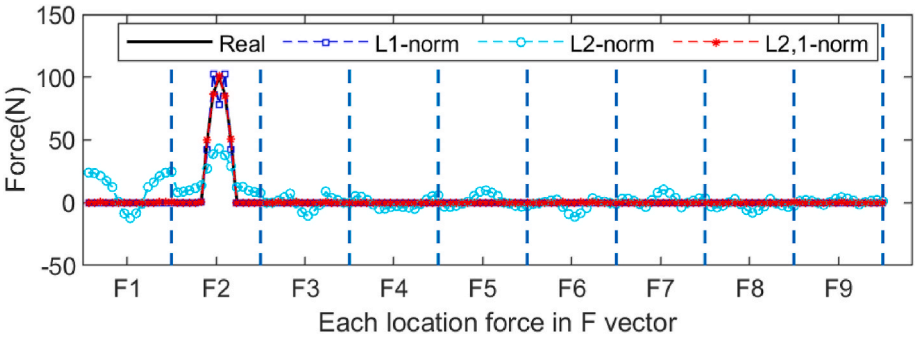

Fig. 6. Identified force vector divided into predefined groups.

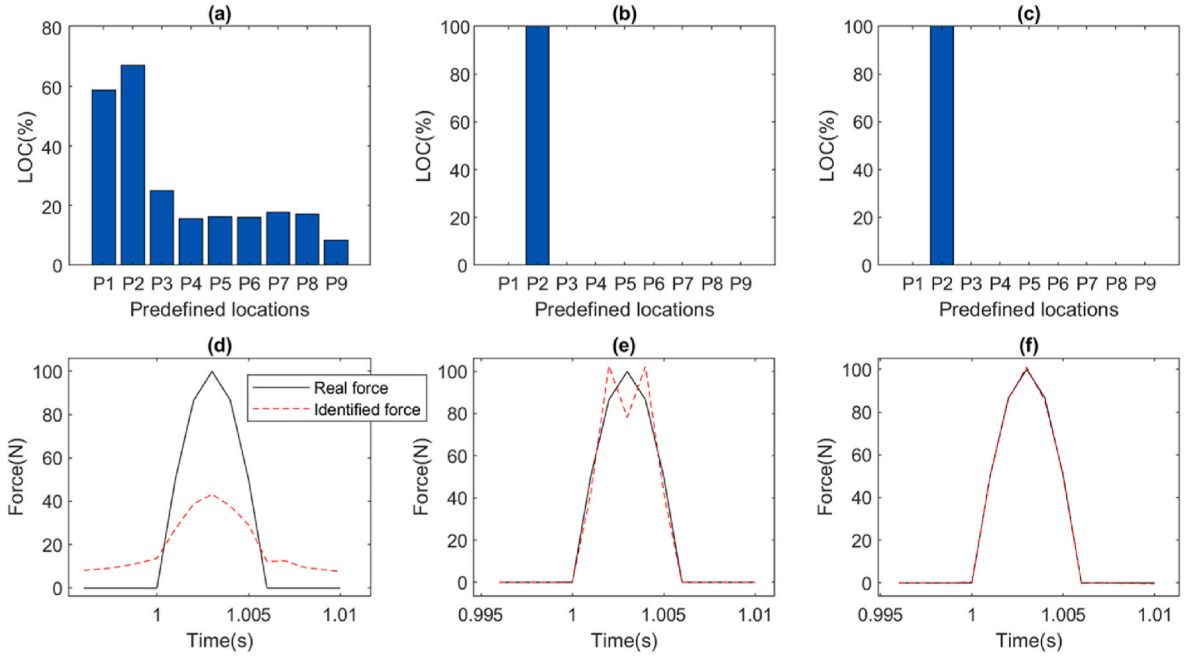

Fig. 7. The results of impact force identification: the localization index results: (a) using L_2-norm regularisation; (b) using L_1-norm regularisation; (c) using $L_{2,1}$-norm regularisation; impact force time history reconstruction at real location results: (d) via L_2-norm regularisation; (e) via L_1-norm regularisation; (f) via $L_{2,1}$-norm regularisation.

Table 1
The LOC values with different sizes of submatrices.

m values	Method	P1	P2	P3	P4	P5	P6	P7	P8	P9
0	L_2-norm	10.5	95.6	11.1	11.9	13.0	12.3	10.0	6.9	3.6
	L_1-norm	0.1	100.0	0.0	0.0	0.0	0.0	0.0	0.0	0.0
	$L_{2,1}$-norm	0.3	100.0	0.2	0.1	0.1	0.2	0.1	0.1	0.1
5	L_2-norm	28.6	27.3	33.8	39.4	47.1	9.3	32.2	40.5	27.7
	L_1-norm	0.0	100.0	0.0	0.0	0.0	0.0	0.0	0.0	0.0
	$L_{2,1}$-norm	0.4	100.0	0.4	0.3	0.2	0.4	0.4	0.3	0.3
10	L_2-norm	28.7	18.8	34.8	41.2	48.4	9.1	33.3	40.5	27.3
	L_1-norm	0.0	100.0	0.0	0.0	0.0	0.0	0.0	0.0	0.0
	$L_{2,1}$-norm	0.7	100.0	0.8	0.3	0.4	0.6	0.6	0.5	0.3
20	L_2-norm	50.5	65.8	27.6	22.1	19.8	22.7	20.6	18.0	14.6
	L_1-norm	0.0	100.0	0.0	0.0	0.0	0.0	0.0	0.0	0.0
	$L_{2,1}$-norm	0.4	100.0	0.5	0.2	0.2	0.4	0.4	0.3	0.2
30	L_2-norm	47.7	64.0	27.2	21.4	20.8	26.0	23.0	22.4	17.1
	L_1-norm	0.0	100.0	0.0	0.0	0.0	0.0	0.0	0.0	0.0
	$L_{2,1}$-norm	0.7	100.0	1.0	0.5	0.5	0.7	0.7	0.6	0.4

Table 2
The RE and PRE values with different sizes of submatrices.

m values	L_2-norm		L_1-norm		$L_{2,1}$-norm	
	RE%	PRE%	RE%	PRE%	RE%	PRE%
0	17.25	20.79	20.15	4.59	0.55	0.07
5	80.51	57.82	20.91	4.90	1.06	0.15
10	97.89	66.12	20.54	4.60	1.96	0.11
20	122.91	72.50	18.25	2.67	3.07	0.86
30	128.45	74.61	16.26	2.16	4.49	1.27

identified results are compared with that by the L_2-norm and L_1-norm regularisation methods. Table 1 shows the LOC values with different sizes of submatrices, e.g. different m values. Table 2 shows the RE and PRE values with different sizes of submatrices. From Table 1, the LOC values at P2 for all m values by the L_1-norm regularisation method and the proposed method are approximate 100 % and the values at other locations are close to zero. The results show that these two methods could identify the location of the impact force with all m values successfully. The L_2-norm regularisation method cannot localize the impact force when $m = 5$ and 10. From Table 2, RE and PRE values by the L_1-norm regularisation method reduces with the increase of the m value, and the values by the proposed method increases slightly with the size of submatrix, e.g. the m value. The RE and PRE values by the proposed method are below 4.5 % and 1.3 % respectively, and they are much smaller than that by the L_1-norm regularisation method, e.g. 20.91 % and 4.90 % respectively. The result indicates the effectiveness and accuracy of the proposed method even with small m value for the partial transfer matrix. There are large errors by the L_2-norm regularisation method. As the above, compared with the L_2-norm and L_1-norm regularisation methods, the proposed method has the best performance for the impact force localization and identification.

In general, the computational cost is directly related to the m value. The computational efficiency for the force identification will be reduced when the m value increases. Although a small m value contains less information, it also reduces the impact of noise. The error of the force identification using the proposed method has a slight increase with the m value. Therefore, a small m value may be considered first for better results in practice.

4.4. Effect of measurement noise

To study the effect of measurement noise, different levels of white noise are added to the calculated response to simulate the polluted measurements, i.e., 1 %, 3 %, 5 %, 10 % and 15 % noise levels are studied. The impact force is the same as that in Section 4.2. One single sensor response is used for the impact force identification. The above-mentioned three regularisation methods are used to identify the impact force based on the partial transfer matrix ($m = 5$) considering different measurement noise. The LOC, RE and PRE values are listed in Tables 3 and 4, respectively. Fig. 8(a), (b) and 8(c) show the LOC, RE and PRE values with different measurement noise levels using three methods. The reconstruction time history results from the responses with different measurement noise levels using three methods are shown in Fig. 8(d), (e) and 8(f) respectively.

Table 4
Identification accuracy index RE and PRE results under different noise levels.

Noise	L_2-norm		L_1-norm		$L_{2,1}$-norm	
	RE%	PRE%	RE%	PRE%	RE%	PRE%
1 %	80.33	57.42	24.97	8.06	0.93	0.32
3 %	80.44	57.43	23.38	6.53	1.02	0.32
5 %	81.11	58.65	21.81	5.88	0.61	0.43
10 %	79.97	59.74	17.87	3.17	4.61	3.30
15 %	81.65	59.85	20.31	3.22	5.55	3.42

From Fig. 8(a) and Table 3, all three methods could indicate the location of the impact force even with 15 % measurement noise. The LOC values by the L_1-norm and $L_{2,1}$-norm regularisation methods are approximate 100 % at the force location and the values are close to zero at other locations. The LOC value by the L_2-norm regularisation method is around 70 % at the force location and the values are not zero at other locations. From Fig. 8(b) and (c), the RE and PRE values are approximate the same for different noise levels. From Table 4, the RE and PRE values of the proposed method are 5.55 % and 3.42 % when the measurement noise is 15 %, and these values are much smaller than that by the L1-norm and L2,1-norm regularisation methods. The results show that the proposed method is much robust to the measurement noise and has the highest accuracy for the impact force reconstruction. Fig. 8(d), (e) and 8 (f) shows the identified impact forces from measurements with different noise levels. The results confirm that the measurement noise does not have large influence on the identified results. There is a big error in the force amplitude by the L_2-norm regularisation method, as shown in Fig. 8(d), and this is due to the smoothing effect of the L_2-norm. From Fig. 8(e), there are some oscillations around the peak of the impact force. The identified results by the proposed $L_{2,1}$-norm regularisation method agree well with the true values as shown in Fig. 8(f).

Table 3
Localization index LOC results under different noise levels.

Impact location		P1	P2	P3	P4	P5	P6	P7	P8	P9
LOC result		LOC_1	LOC_2	LOC_3	LOC_4	LOC_5	LOC_6	LOC_7	LOC_8	LOC_9
1 %	L_2-norm	56.2	73.7	16.9	13.1	15.9	15.9	15.6	12.6	6.8
	L_1-norm	0.0	100.0	0.0	0.0	0.0	0.0	0.0	0.0	0.0
	$L_{2,1}$-norm	0.1	100.0	0.1	0.0	0.1	0.1	0.1	0.1	0.1
3 %	L_2-norm	56.2	73.7	16.7	13.2	15.9	15.9	15.5	12.6	6.9
	L_1-norm	0.0	100.0	0.0	0.0	0.0	0.0	0.0	0.0	0.0
	$L_{2,1}$-norm	0.2	100.0	0.2	0.1	0.1	0.2	0.1	0.2	0.1
5 %	L_2-norm	56.1	73.8	16.9	13.0	16.0	16.1	15.6	12.6	6.8
	L_1-norm	0.1	100.0	0.0	0.0	0.0	0.0	0.0	0.0	0.0
	$L_{2,1}$-norm	0.2	100.0	0.2	0.1	0.1	0.1	0.1	0.1	0.1
10 %	L_2-norm	56.0	73.6	17.4	12.9	15.9	16.5	15.7	12.8	6.7
	L_1-norm	1.2	100.0	0.8	0.2	1.0	0.0	0.6	0.2	0.3
	$L_{2,1}$-norm	0.9	100.0	0.9	0.5	0.7	0.6	0.6	0.5	0.6
15 %	L_2-norm	55.9	73.5	17.3	13.2	16.0	16.3	15.8	13.0	7.2
	L_1-norm	0.8	100.0	0.9	0.0	0.7	0.7	0.2	0.0	0.1
	$L_{2,1}$-norm	1.2	100.0	1.2	0.8	0.5	0.9	0.9	0.7	0.8

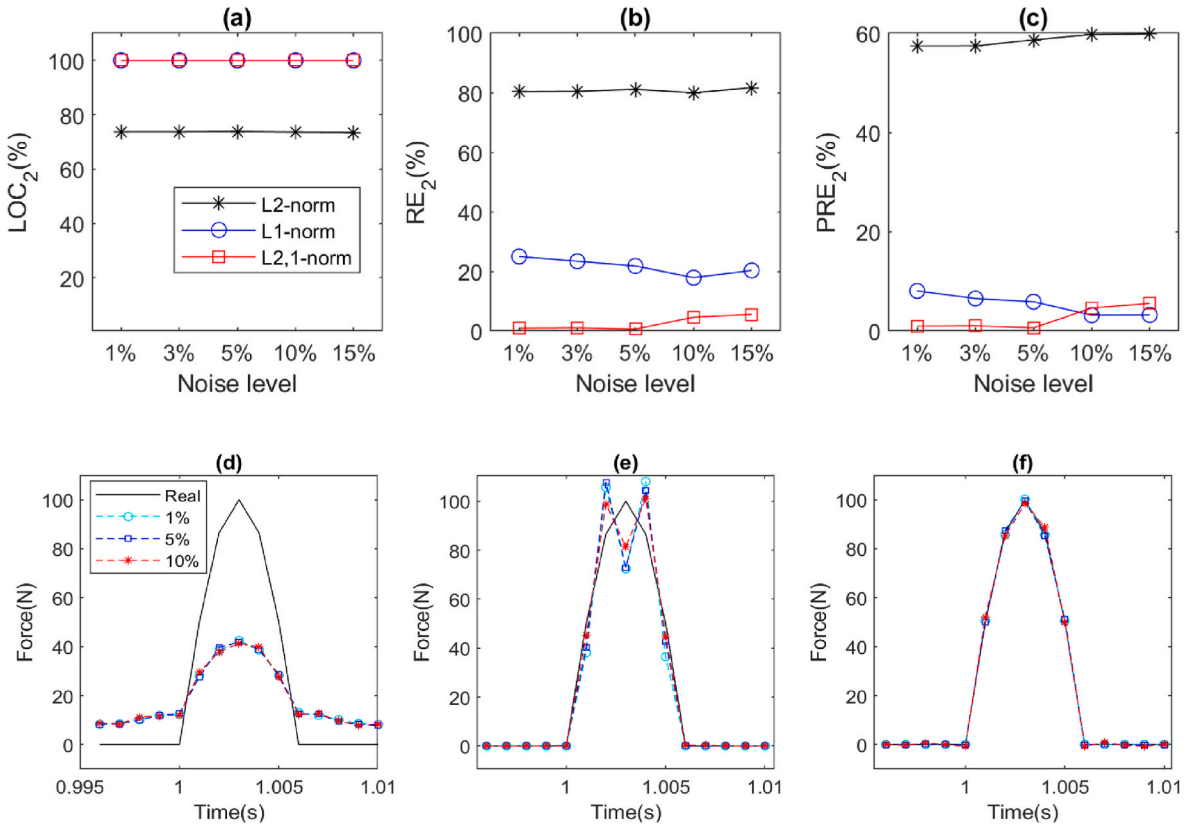

Fig. 8. The results of impact force identification under different noise effect: The identification index results: (a) localization index LOC; (b) identification accuracy index RE; (c) identification accuracy index PRE; impact force time history reconstruction at real location results under 1 %, 5 % and 10 % noise effect results: (d) via L_2-norm regularisation; (e) via L_1-norm regularisation; (f) via $L_{2,1}$-norm regularisation.

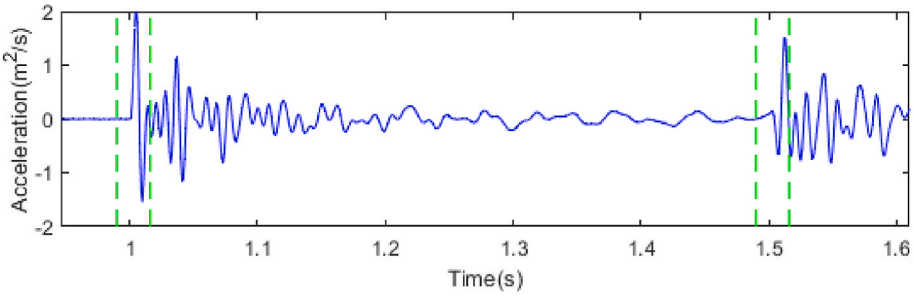

Fig. 9. Accelerations for estimation of two intervals related to impact forces.

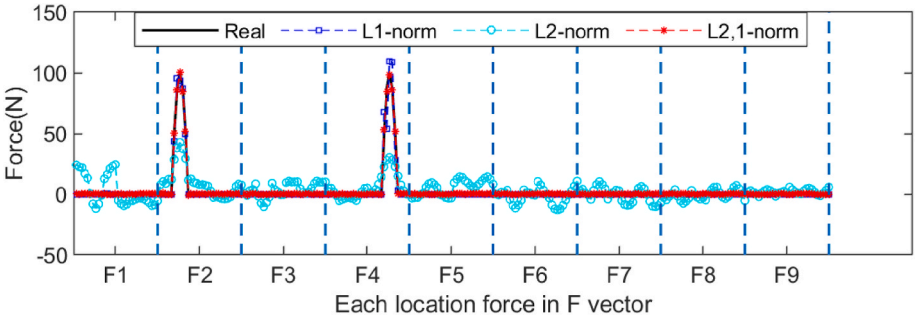

Fig. 10. Identified force vector for double impact divided into predefined groups.

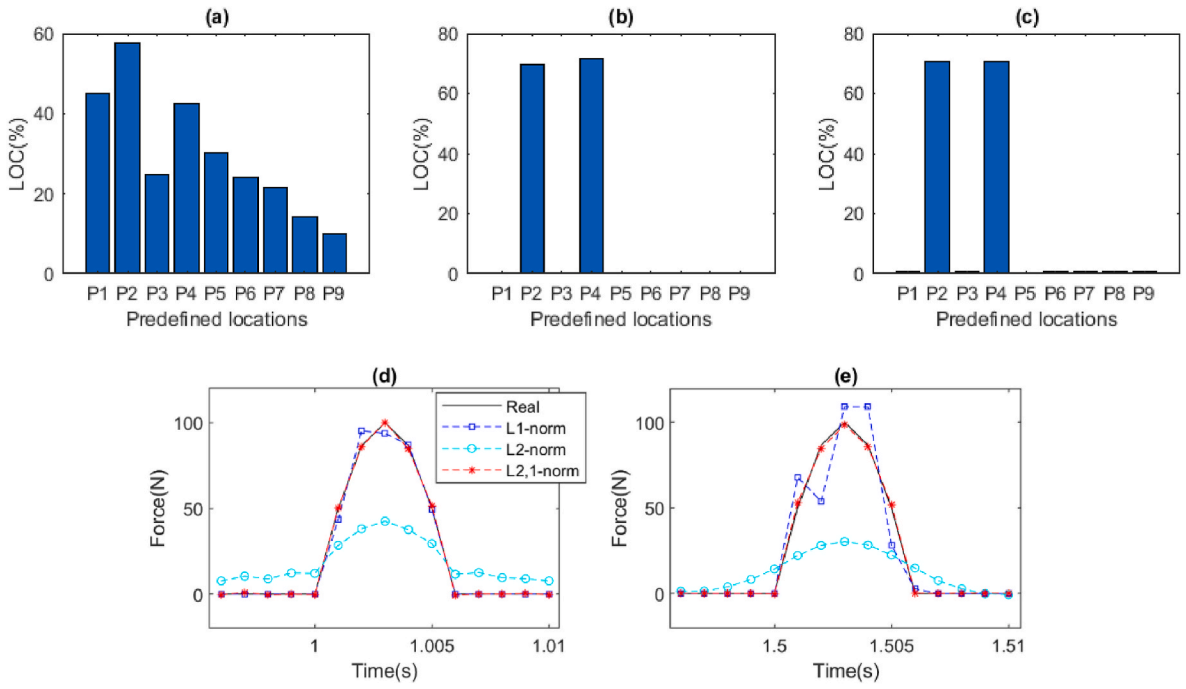

Fig. 11. The results of two impact force identification: the localization index results: (a) using L_2-norm regularisation; (b) using L_1-norm regularisation; (c) using $L_{2,1}$-norm regularisation; impact force time history reconstruction at real location results: (d) identified impact force at P2; (e) identified impact force at P4.

4.5. Multiple impact force identification with one single sensor

In practice, multiple impact forces usually appear at different locations asynchronously. The identification of two and three impact forces using the proposed method is studied in this section. For the case with two impact forces, these impact forces are applied at the locations P2 and P4 separately. The response of one single sensor (Y_1) shown in Fig. 9 is used. 5 % noise is added to the response to simulate the polluted measurement. The interval between two adjacent green dash lines is obtained as $m = 5$ in Fig. 9 and the corresponding transfer submatrix is selected for the impact force localization and reconstruction. There are two intervals corresponding to two impact forces in Fig. 9.

The identified force vector results based on the proposed method are illustrated in Fig. 10. The corresponding localization results of two impact forces by three methods are shown in Fig. 11(a), (b) and 11(c) respectively. The reconstructed time histories of two impact force are shown in Fig. 11(d) and (e) respectively. The LOC, RE and PRE values are listed in Tables 5 and 6. From Fig. 10, the locations of two impact forces at P2 and P4 are identified successfully by the L_1-norm regularisation method and the proposed $L_{2,1}$-norm regularisation method. The identified result by the L_2-norm regularisation method contains highly oscillatory false components at other locations and these oscillations affect the accuracy of the impact force identification. From Table 5, the LOC values at locations of these two impact forces are 70 % or above by the L_1-norm regularisation method and the proposed $L_{2,1}$-norm regularisation method and the results show that the impact forces could be accurately located. The LOC values at locations of two impact forces by the L_2-norm regularisation method are only 57.5 % and 42.5 % respectively. Fig. 11(d) and (e) show the identified impact force time histories by three methods. The identified results of two impact forces by the proposed $L_{2,1}$-norm regularisation method are close to the true values. The identified result of the impact force at P2 by the L_1-norm regularisation method is close to the true value and there are some

Table 6
Identification accuracy index RE and PRE results for different number of impact force.

Impact number	Impact position	L_2-norm		L_1-norm		$L_{2,1}$-norm	
		RE%	PRE %	RE%	PRE %	RE %	PRE %
1	P2	81.11	58.65	21.81	5.88	0.61	0.43
2	P2	99.78	57.20	4.59	4.39	1.60	0.69
	P4	46.87	69.73	11.66	8.47	1.74	1.32
3	P2	59.11	58.61	4.07	2.21	2.05	0.27
	P4	62.21	69.56	8.10	6.21	1.63	0.95
	P6	40.34	64.19	6.87	5.36	1.33	1.06

Table 5
Localization index LOC results for different number of impact force.

Impact location		P1	P2	P3	P4	P5	P6	P7	P8	P9
1	L_2-norm	56.1	73.8	16.9	13.0	16.0	16.1	15.6	12.6	6.8
	L_1-norm	0.1	100.0	0.0	0.0	0.0	0.0	0.0	0.0	0.0
	$L_{2,1}$-norm	0.2	100.0	0.2	0.1	0.1	0.1	0.1	0.1	0.1
2	L_2-norm	45.2	57.5	24.7	42.5	30.0	23.9	21.4	14.3	9.9
	L_1-norm	0.0	69.9	0.0	71.6	0.0	0.2	0.0	0.0	0.0
	$L_{2,1}$-norm	0.7	70.7	0.8	70.7	0.4	0.7	0.6	0.6	0.6
3	L_2-norm	39.0	48.2	23.1	38.9	26.7	44.8	26.9	17.4	18.9
	L_1-norm	0.2	57.2	0.3	57.7	0.0	58.3	0.7	0.2	0.1
	$L_{2,1}$-norm	0.5	57.8	0.6	57.7	0.2	57.6	0.5	0.4	0.4

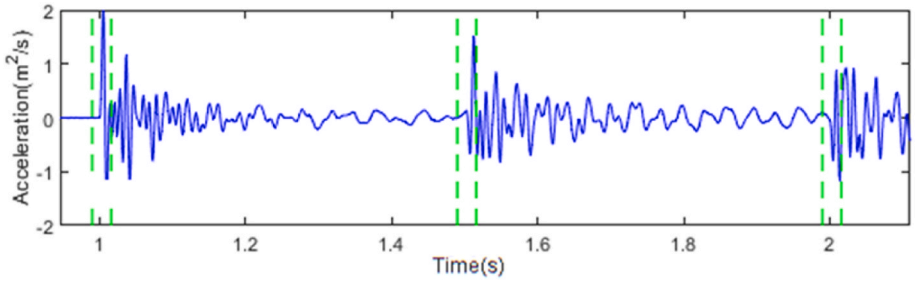

Fig. 12. Acceleration time history for triple excitations interval determination.

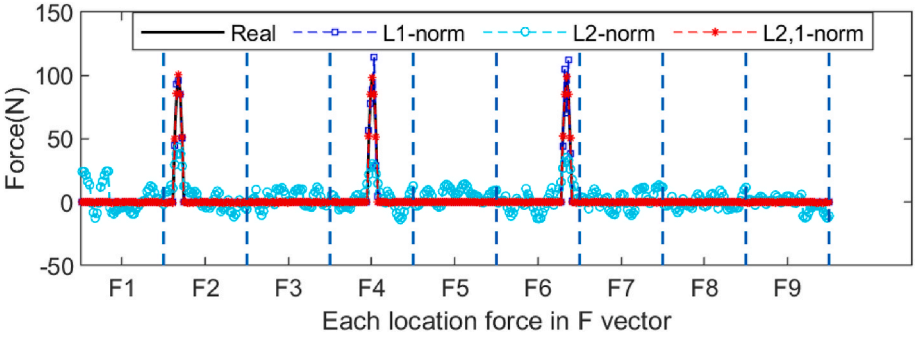

Fig. 13. Identified force vector for triple impacts divided into predefined groups.

oscillations at the identified result of the impact force at P4. This is probably induced by the initial response condition for the second impact force. For the first impact force conducted at P2, the initial response is zero. While for the second impact force at P4, the initial response is non-zero and it may affect the second force identification. There is no effect by the proposed $L_{2,1}$-norm regularisation method as shown in Fig. 11(d) and (e). Accurate force time history for both impact forces are obtained using the proposed method.

For the case of three impact force identification, three impact forces are applied at locations P2, P4 and P6 separately. One single sensor (Y1) response shown in Fig. 12 is employed, and 5 % noise is added to the response to simulate the polluted measurement. Three intervals

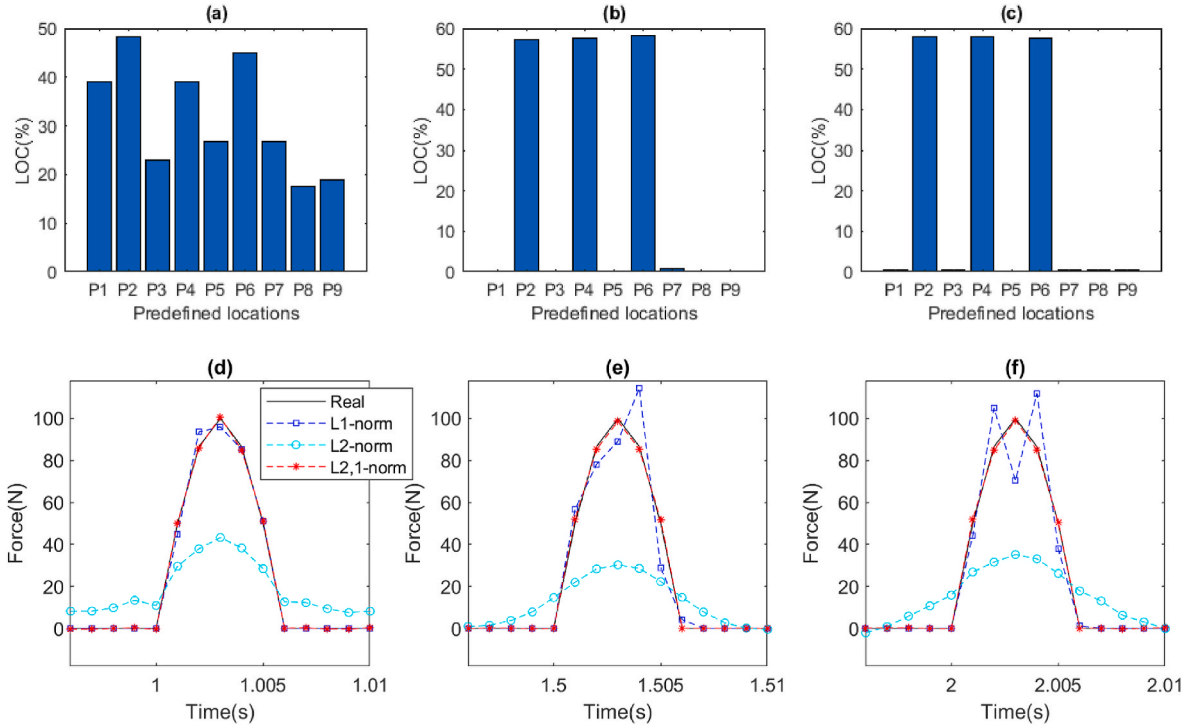

Fig. 14. The results of triple impact force identification: the localization index results: (a) using L_2-norm regularisation; (b) using L_1-norm regularisation; (c) using $L_{2,1}$-norm regularisation; impact force time history reconstruction at real location results: (d) identified impact force at P2; (e) identified impact force at P4; (e) identified impact force at P6.

indicated by green dash lines in Fig. 12 associated transfer submatrices are selected for three impact force localization and reconstruction.

Three forces with the same amplitude and distance are used to verify the proposed method. The identified force vector results by three methods are illustrated in Fig. 13. The corresponding localization results by three methods are shown in Fig. 14(a) and (b) and 14 (c) respectively. The reconstructed time histories of three impact forces are shown in Fig. 14(d), (e) and 14(f) respectively. The corresponding LOC, RE and PRE values are listed in Tables 5 and 6 From Figs. 13 and 14, and Tables 5 and 6, three impact force forces are located successfully by the L_1-norm regularisation method and the proposed $L_{2,1}$-norm regularisation method and the identified results of three impact forces by the proposed method are all close to the true values. The proposed transfer submatrix based $L_{2,1}$-norm regularisation method has the best performance on multiple impact force localization and reconstruction.

5. Experimental validation

5.1. Experimental setup

To further verify the effectiveness and applicability of the proposed method, the experimental study is performed on a steel-concrete composite bridge model shown in Fig. 15. As shown in Fig. 16, 28 possible impact force locations are predefined and labelled from S1 to S14 and N1 to N14. The impact hammer (PCB 086D20 with sensitivity 0.23 mV/N) is used for the excitation. NI data acquisition system is used to record the impact force and acceleration response data with a sampling frequency 1000Hz. The acceleration response from A2 is used for the impact force identification. Single force (conducted at S4) identification and two force (conducted at S4 and S6) identification are conducted in this section. The transfer matrix can be constructed according to the

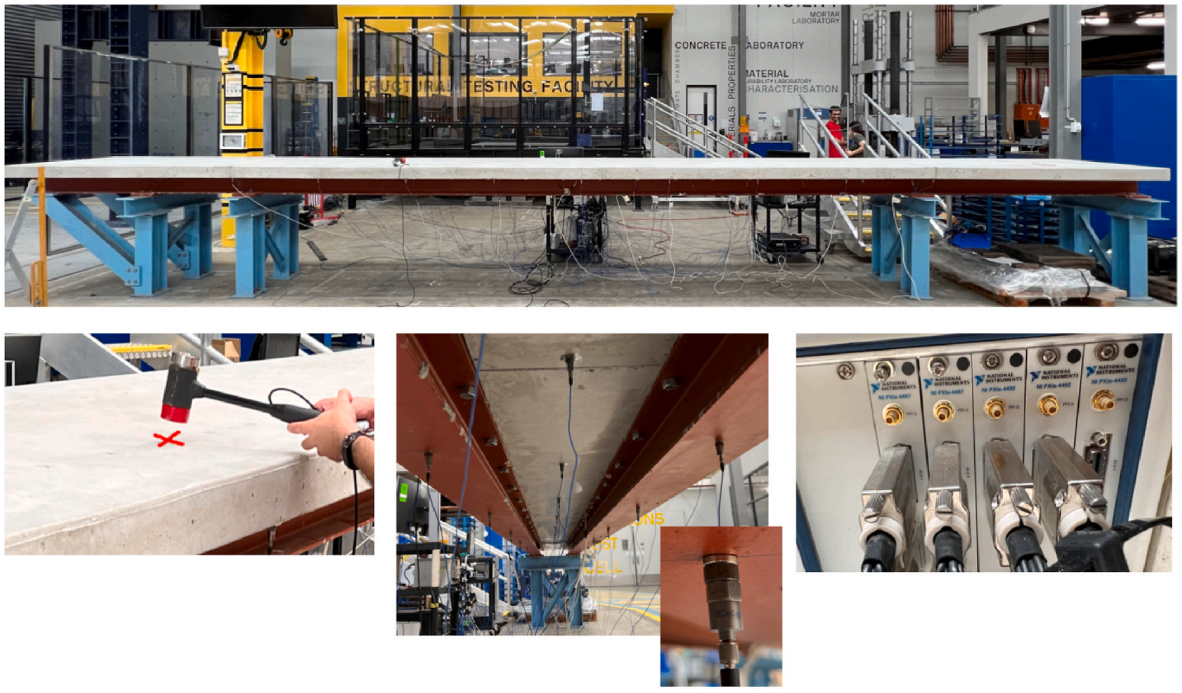

(a) Experimental setup

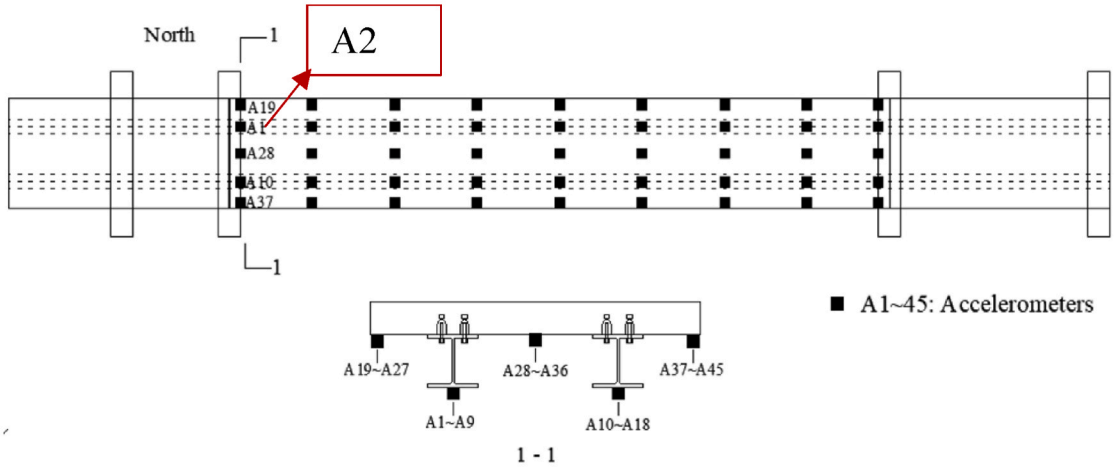

(b) Sensor instrumentation

Fig. 15. Experimental model and acquisition equipment.

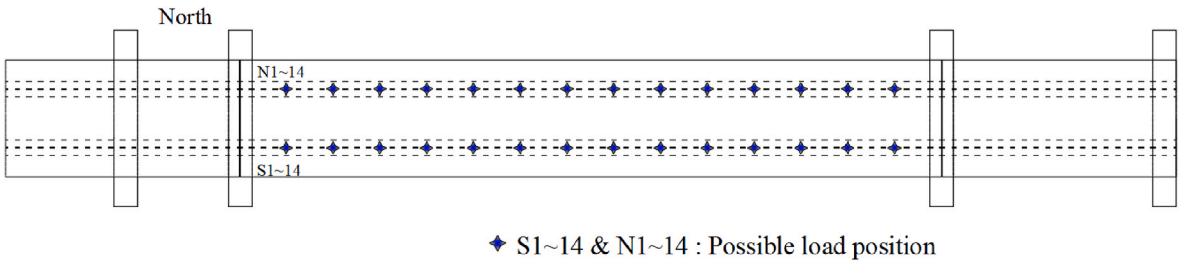

Fig. 16. Predefined possible load position in the experiment model.

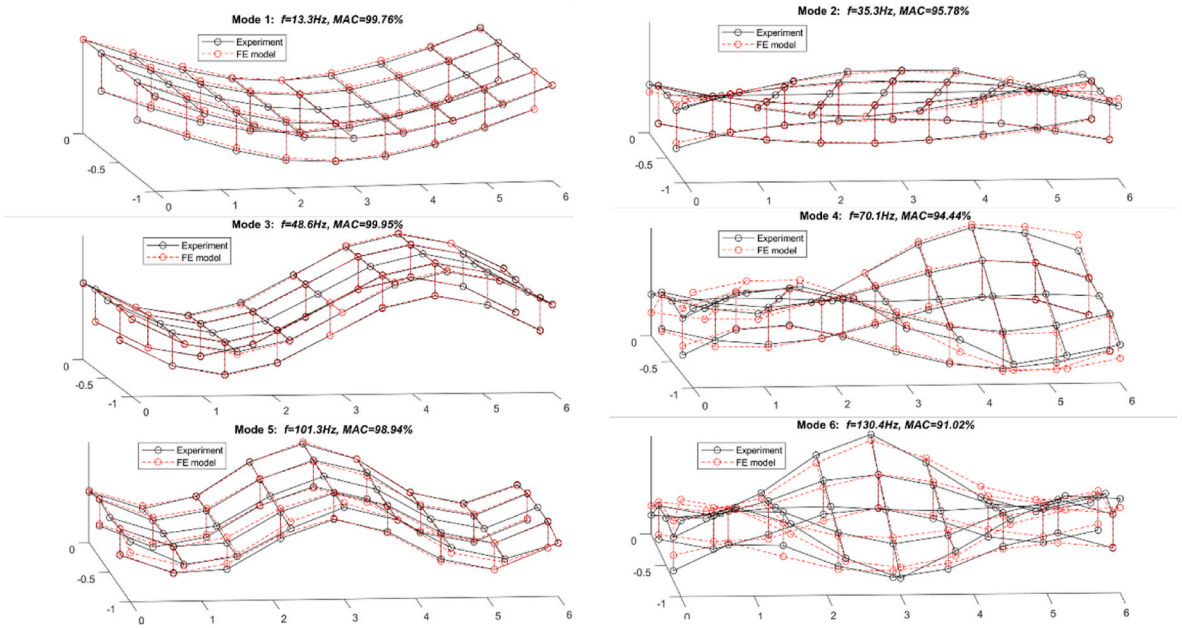

Fig. 17. Modal parameters of the beam from experimental model and FE model.

modal test. The identified modal results compared to its finite element modelling are shown in Fig. 17. The transfer submatrix associated with the impact force time interval could be selected for the loading interval force identification.

5.2. Results and discussions

The proposed transfer submatrix-based group sparse method is used to identify the impact force and the results are compared with that by the L_2-norm and L_1-norm regularisation methods. Fig. 18 shows the single impact force localization and reconstruction results from one single response. Fig. 18(a), (b) and 18(c) show the identified location of the impact force using three methods respectively. Fig. 18(d), (e) and 18(f) show the corresponding identified impact force time histories respectively. From Fig. 18(a)–(c), the location of the impact force is clearly indicated by the peaks of the results by the L_1-norm regularisation method and $L_{2,1}$-norm regularisation method. There is no clear peak by the L_2-norm regularisation method and it shows that the method fails to obtain the clear location information. From Fig. 18(d)–(f), the identified result by the proposed method is much closer to the true value compared with that by other two methods. From Fig. 18(b) and (e), it can also see that the impact force localization and time history identification is less accurate by the L_1-norm regularisation method comparing with the proposed method.

The same accelerometer (A2) is used to identify two impact forces at S4 and S6 separately. The LOC values by three methods are shown in Fig. 19(a), (b) and 19(c) respectively. The reconstructed time histories of these two impact forces are shown in Fig. 19(e) and (f). Fig. 19(a), (d) and 19(e) show that two impact forces are not able to be located and reconstructed by the L_2-norm regularisation method. Fig. 19(b) shows that two impact forces could be located correctly and the LOC value for the second force is less than 50 %. From Fig. 19(d) and (e), the identified first impact force is larger than the true value and the identified second impact force is smaller than the true value by the L_1-norm regularisation method. That means the first force is overestimated and the second one is underestimated. On the other hand, by the proposed $L_{2,1}$-norm regularisation method, these two impact forces are clearly located by two peaks and the identified results are much close to the true values. The results show that the proposed method has good robustness and accuracy for two impact force identification of complex bridge structures.

6. Conclusions

In this paper, the transfer submatrix-based group sparse regularisation method for multiple impact force localization and reconstruction has been developed. Based on the intrinsic feature of impact force, the transfer submatrix associated with the impact excitation time interval could be constructed for the loading interval force identification. By this method, the dimension of the inverse problem can be dramatically decreased, and the computational efficiency can be significantly improved. It could also reduce the ill-posedness of the inverse problem, especially when the number of sensors is less than the number of impact forces. The force group could be grouped based on the potential force locations. The proposed method could obtain stable and accurate results

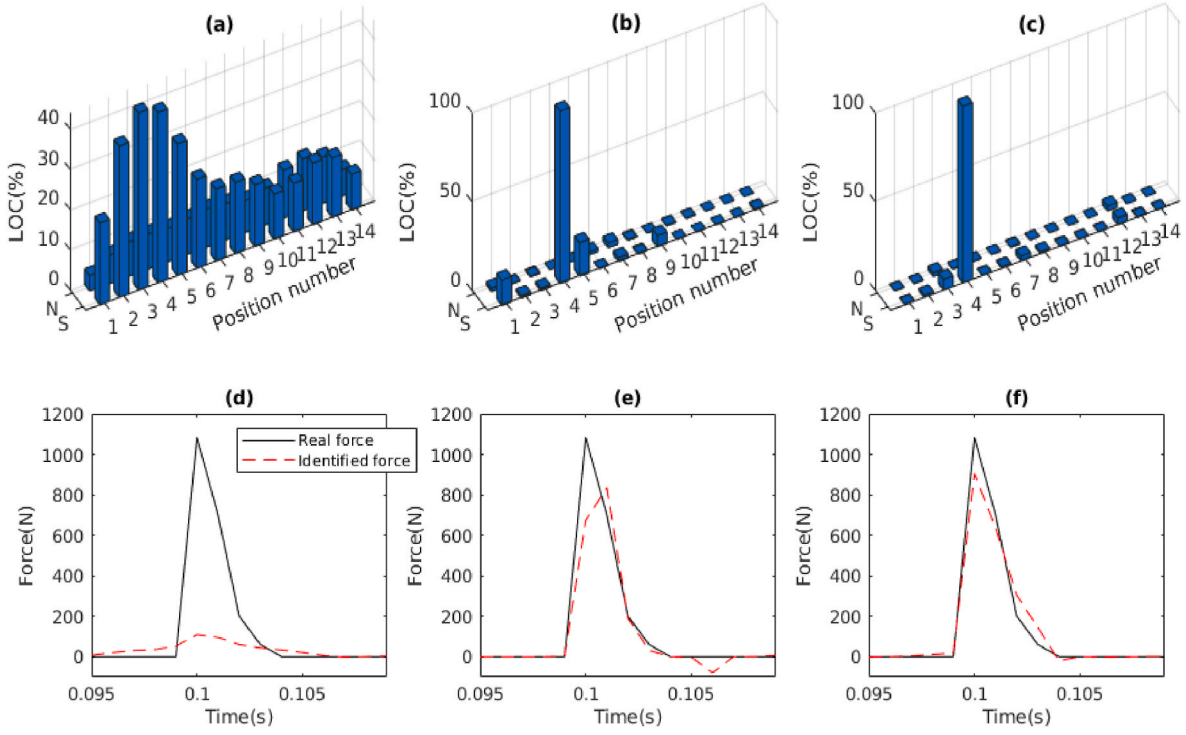

Fig. 18. Experimental results of single impact force identification at location S4: the localization index results: (a) using L_2-norm regularisation; (b) using L_1-norm regularisation; (c) using $L_{2,1}$-norm regularisation; impact force time history reconstruction at real location results: (d) via L_2-norm regularisation; (e) via L_1-norm regularisation; (f) via $L_{2,1}$-norm regularisation.

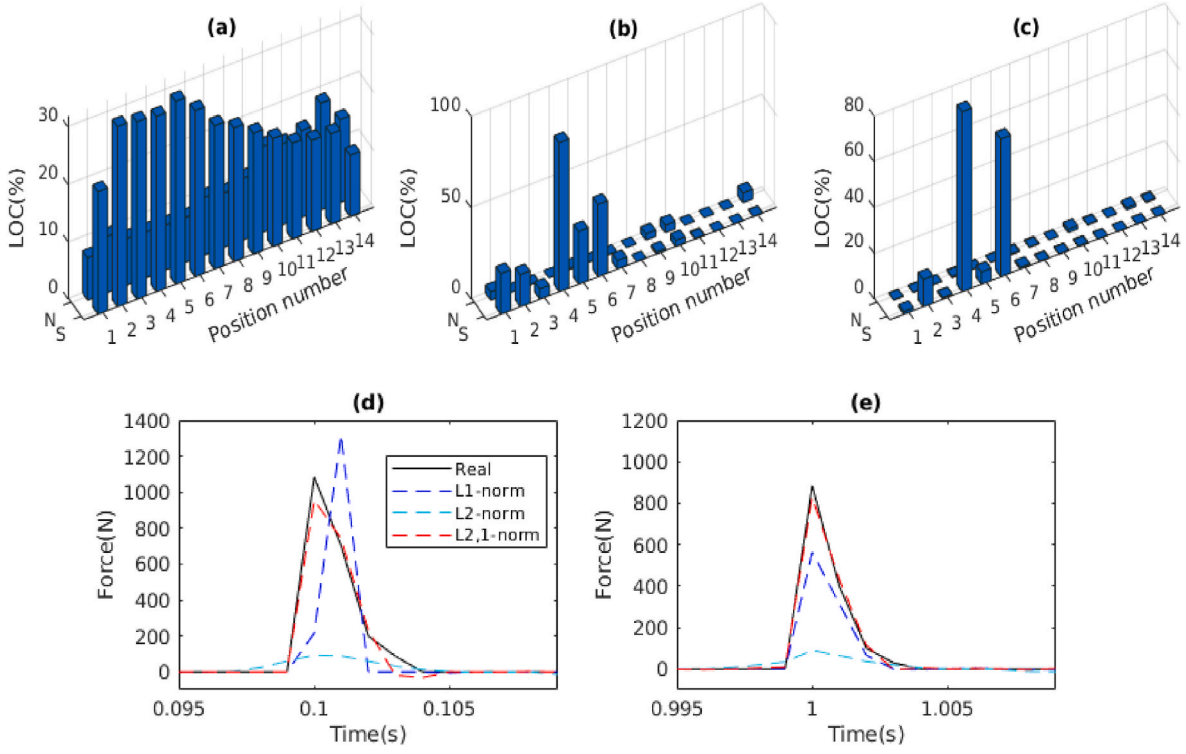

Fig. 19. Experimental results of double impact force identification: the localization index results: (a) using L_2-norm regularisation; (b) using L_1-norm regularisation; (c) using $L_{2,1}$-norm regularisation; impact force time history reconstruction at real location results: (d) identified impact force at S4; (e) identified impact force at S6.

based on the structured group sparsity in the force vector. The group sparse regularisation method based on the $L_{2,1}$-norm penalty is validated and compared with the L_1-norm regularisation method and the L_2-norm regularisation method numerically and experimentally. In the numerical study, determination of the submatrix, noise effect and multiple impacts identification are investigated using one single sensor response. Comparing with the L_1-norm and L_2-norm regularisation methods, the proposed transfer submatrix-based group sparse regularisation method has the best performance on the multiple impact force localization and time history reconstruction.

The proposed method adopted the transfer submatrix, and the computational efficiency and accuracy of force identification are significantly increased, especially for large-scale structures in practice. The performance of the proposed method is verified using the numerical and laboratory experimental studies. In this study, the transfer matrix is constructed using numerical modelling or laboratory modal testing. Further verification is needed for practical applications in real-time monitoring systems of complex structures in operational environment.

CRediT authorship contribution statement

Bing Zhang: Writing – review & editing, Writing – original draft, Validation, Software, Methodology, Formal analysis, Conceptualization. **Xinqun Zhu:** Writing – review & editing, Supervision, Methodology. **Zihao He:** Writing – review & editing. **Jianchun Li:** Writing – review & editing, Supervision.

Declaration of competing interest

The authors declared that they have no conflicts of interest to this work. We declare that we do not have any commercial or associative interest that represents a conflict of interest in connection with the work submitted.

References

Armijo, L., 1966. Minimization of functions having Lipschitz-continuous first partial derivatives. Pac. J. Math. 16, 1–3. https://doi.org/10.2140/pjm.1966.16.1.

Barzilai, J., Borwein, J., 1988. Two point step size gradient methods. IMA J. Numer. Anal. 8, 141–148. https://doi.org/10.1093/imanum/8.1.141.

Feng, W., Li, Q., Lu, Q., Li, C., Wang, B., 2021. Group relevance vector machine for sparse force localization and reconstruction. Mech. Syst. Signal Process. 161. https://doi.org/10.1016/j.ymssp.2021.107900.

Goutaudier, D., Gendre, D., Kehr-Candille, V., Ohayon, R., 2020. Single-sensor approach for impact localization and force reconstruction by using discriminating vibration modes. Mech. Syst. Signal Process. 138, 106534. https://doi.org/10.1016/j.ymssp.2019.106534.

Inoue, H., Harrigan, J.J., Reid, S.R., 2001. Review of inverse analysis for indirect measurement of impact force. Appl. Mech. Rev. 54 (6), 503–524. https://doi.org/10.1115/1.1420194.

Jacquelin, E., Bennani, A., Hamelin, P., 2003. Force reconstruction: analysis and regularization of a deconvolution problem. J. Sound Vib. 265 (1), 81–107. https://doi.org/10.1016/S0022-460X(02)01441-4.

Jia, Y., Yang, Z., Song, Q., 2015. Experimental study of random dynamic loads identification based on weighted regularization method. J. Sound Vib. 342, 113–123. https://doi.org/10.1016/j.jsv.2014.12.010.

Kalhori, H., Alamdari, M.M., Ye, L., 2018. Automated algorithm for impact force identification using cosine similarity searching. Measurement 122, 648–657. https://doi.org/10.1016/j.measurement.2018.01.016.

Khanam, S., Dutt, J.K., Tandon, N., 2015. Impact force based model for bearing local fault identification. J. Vib. Acoust. 137 (5), 051002. https://doi.org/10.1115/1.4029988.

LeClerc, J.R., Worden, K., Staszewski, W.J., Haywood, J., 2007. Impact detection in an aircraft composite panel—a neural-network approach. J. Sound Vib. 299 (3), 672–682. https://doi.org/10.1016/j.jsv.2006.07.019.

Li, Q., Lu, Q., 2016. Impact localization and identification under a constrained optimization scheme. J. Sound Vib. 366, 133–148. https://doi.org/10.1016/j.jsv.2015.12.010.

Liu, R., Dobriban, E., Hou, Z., Qian, K., 2021. Dynamic load identification for mechanical systems: a review. Arch. Comput. Methods Eng. 29 (2), 831–863. https://doi.org/10.1007/s11831-021-09594-7.

Liu, J., Qiao, B., Chen, Y., Zhu, Y., He, W., Chen, X., 2022. Impact force reconstruction and localization using nonconvex overlapping group sparsity. Mech. Syst. Signal Process. 162, 107983. https://doi.org/10.1016/j.ymssp.2021.107983.

Meier, L., Van De Geer, S., Bühlmann, P., 2008. The group lasso for logistic regression. J. Roy. Stat. Soc. B 70, 53–71. https://doi.org/10.1111/j.1467-9868.2007.00627.x.

Park, J., Ha, S., Chang, F.-K., 2009. Monitoring impact events using a system-identification method. AIAA J 47 (9), 2011–2021. https://doi.org/10.2514/1.34895.

Qiao, B., Liu, J., Liu, J., Yang, Z., Chen, X., 2019a. An enhanced sparse regularization method for impact force identification. Mech. Syst. Signal Process. 126, 341–367. https://doi.org/10.1016/j.ymssp.2019.02.039.

Qiao, B., Mao, Z., Liu, J., Zhao, Z., Chen, X., 2019b. Group sparse regularization for impact force identification in time domain. J. Sound Vib. 445, 44–63. https://doi.org/10.1016/j.jsv.2019.01.004.

Qiu, B., Zhang, M., Xie, Y., Qu, X., Li, X., 2019. Localisation of unknown impact loads on a steel plate using a pattern recognition method combined with the similarity metric via structural stress responses in the time domain. Mech. Syst. Signal Process. 128, 429–445. https://doi.org/10.1016/j.ymssp.2019.04.015.

Sanchez, J., Benaroya, H., 2014. Review of force reconstruction techniques. J. Sound Vib. 333 (14), 2999–3018. https://doi.org/10.1016/j.jsv.2014.02.025.

Wambacq, J., Maes, K., Rezayat, A., Guillaume, P., Lombaert, G., 2019. Localization of dynamic forces on structures with an interior point method using group sparsity. Mech. Syst. Signal Process. 115, 593–606. https://doi.org/10.1016/j.ymssp.2018.06.006.

Wang, B.T., Chiu, C.-H., 2003. Determination of unknown impact force acting on a simply supported beam. Mech. Syst. Signal Process. 17 (3), 683–704. https://doi.org/10.1006/mssp.2001.1463.

Zhu, X., Law, S., 2002. Moving loads identification through regularization. J. Eng. Mech. 128 (9), 989–1000. https://doi.org/10.1061/(ASCE)0733-9399(2002)128:9(989).